Astron. Astrophys. 331, 70–80 (1998)

ASTRONOMY
AND
ASTROPHYSICS

Infrared array photometry of bulge globular clusters

I. Combined ground based JK and HST VI photometry of NGC 6553⋆

M.D. Guarnieri[1,2], **S. Ortolani**[3], **P. Montegriffo**[4], **A. Renzini**[1,4], **B. Barbuy**[5], **E. Bica**[6], **and A. Moneti**[7]

[1] European Southern Observatory, Karl-Schwarzschild 2, D-85748 Garching b. München, Germany
[2] Osservatorio Astronomico di Pino Torinese, I-10025 Torino, Italy
[3] University of Padova, Vicolo dell'Osservatorio 5, I-35123 Padova, Italy
[4] Dipartimento di Astronomia di Bologna, Bologna, Italy
[5] IAG-USP, CP 9638, 01065-970 São Paulo, Brazil
[6] UFRGS, CP 15051, 91501-970 Porto Alegre, Brazil
[7] SERCO/ESA-Astrophysics Division, Noordwijk, The Netherlands

Received 26 July 1996 / Accepted 6 January 1997

Abstract. JK infrared photometry for the bulge globular cluster NGC 6553, combined with high resolution visual VI observations are presented and discussed in connection with the bulge metal rich population. The infrared data were taken with IRAC2 at ESO 2.2m telescope while the optical counterparts are from Hubble Space Telescope (HST).

We find a mean magnitude for the horizontal branch of V_{HB} = 16.92, and K_{HB} = 12.42 ± 0.01. Assuming a reddening of $E(B-V)$ = 0.7, the mean distance modulus is $(m-M)_0$ = 13.6 giving an heliocentric distance of 5.2 Kpc. This distance is slightly higher than that previously published by Ortolani et al. (1990, hereafter OBB90).

The brightest giants have been detected at $K \sim 6.5$ and $(V-K)$ = 13.10 transforming to $M_K = -7.34$ and $(V-K)_0$ = 11.20, which are exceptionally high values for a globular cluster.

The metallicity has been found to be consistent with previous values and an average of $[Fe/H] = -0.22 \pm 0.05$ has been adopted. The helium abundance estimated via the R' method yields $Y_p \sim 0.28 \pm 0.03$.

Key words: globular clusters: NGC 6553 – Galaxy: center – blue stragglers – HR diagram

1. Introduction

The Galactic bulge plays an important rôle in the understanding of the evolution of our Galaxy. In spite of a number of recent claims on the formation of the galactic bulge as a late event in the Galaxy evolution (Raha et al. 1991), there is growing evidence for an old galactic bulge coeval with the halo (Ortolani et al. 1995). Precise measurements of luminosity, colours and metallicities of bulge stars are hampered by crowding, differential reddening, different distances along the line of sights and contamination due to foreground bright disk main sequence stars. However, the bulge region contains a number of peculiar globular clusters with a very high metal content and a colour magnitude diagram (CMD) morphology very similar to that of the field population.

In the optical range, their CMDs are dominated by blanketing effects, with anomalous tilted horizontal branches (HB) and a turnover of the giant branch (Ortolani et al. 1990, 1991, 1992, 1993a, 1993b, Bica et al. 1991) so that the brightest stars are not the coolest asymptotic giant branch (AGB) ones. In spite of the high luminosity foreseen by the theoretical models, the brightest stars are in general fainter than those in metal poor clusters.

In the infrared, instead, the blanketing effects due to the high metallicity as well as those due to reddening are much less important. The AGB stars are considerably brighter than disk main sequence stars, reducing the contamination effects.

The main goal of this paper is to provide IR metal rich population template CMDs for further bulge population studies. A much better baseline for the temperature of the giants is also provided by combining optical and infrared photometry. This is a fundamental item for spectroscopic studies.

By combining optical and IR data it is also possible to obtain very useful colour indices, like $(V-K)$, which is an excellent indicator of the effective temperature (T_e). This colour is not

Send offprint requests to: Maria Donata Guarnieri

⋆ Based on observations obtained at ESO-La Silla, Chile and with the NASA/ESA Hubble Space Telescope, obtained at the Space Telescope Science Institute, operated by AURA Inc. under contract to NASA.
Appendix only available in electronic form at the CDS (Strasbourg) via anonymous ftp to cdsarc.u-strasbg.fr (130.79.128.5) or via http://cdsweb.u-strasbg.fr/Abstract.html

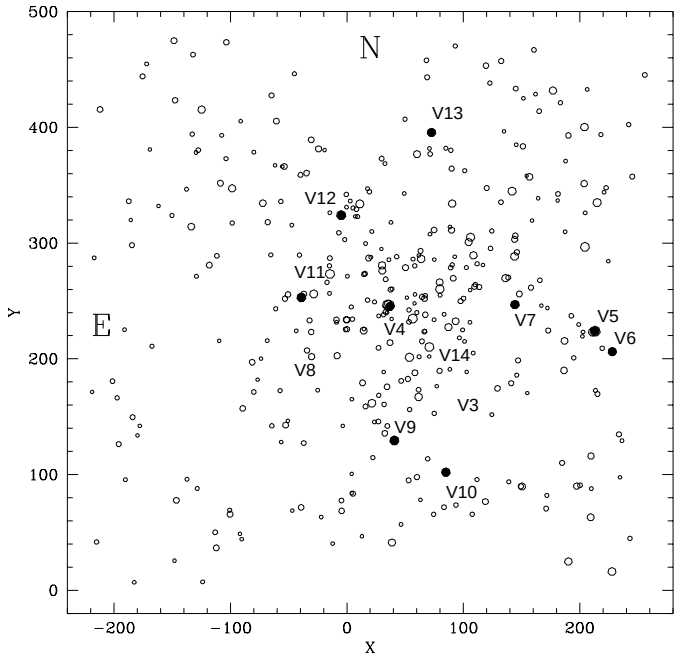

Fig. 1. Composite image of the covered field. North is up and East is to the left. Filled circles indicate the position of the variable stars in common with Lloyd Evans and Menzies (1973, hereafter LM73) and Sawyer Hogg (1973, hereafter SH73). Coordinates are in pixels (0.49 arcsec $pixel^{-1}$).

affected by the saturation effects at low temperatures, contrary to those in the optical (Guarnieri et al. 1992; Ferraro et al. 1994).

In this work we present combined visual and near-infrared CMDs for NGC 6553 ($\alpha = 18^h05^m11^s$; $\delta = -25^o55'06''$ (1950.0)). This cluster is located at a very low galactic latitude ($l = 5^o.25$, $b = -3^o.02$) and is metal-rich ($[Fe/H] = -0.2^{+0.2}_{-0.4}$) (Barbuy et al. 1992). Thus it is a key cluster for a better understanding of metal-rich stellar populations.

In Sect. 2 the observations and calibrations are described. In Sect. 3 comparison is made with previous data. In Sect. 4 the CMDs are presented. In Sect. 5 we discuss variable stars. In Sect. 6 the cluster parameters are analysed. Finally the conclusions are drawn in Sect. 7.

2. Observations and data reductions

Infrared observations have been carried out on June 11, 1992 using the ESO Rockwell NICMOS-3 (HgCdTe, 256×256 pixels) infrared camera IRAC-2 (cutoff wavelength at 2.5 μm , Moorwood et al. 1992) mounted on the Max Planck Institute/ESO 2.2m telescope at La Silla (Chile), with the image scales of 0.27" and 0.49" for both standard J (1.25 μm) and K (2.19 μm) filters. Through each filter, we obtained a high resolution image (first magnification value) of the cluster center, and four partially overlapping images covering a $\sim 2' \times 2'$ square region centered on the cluster core (second magnification). The total field covered is $\sim 4 \times 4$ arcmin^2. In Fig. 1 we show the computer map of the stars detected in the IR survey ($K < 12$ mag).

Separate sky frames located at $\sim 10'$ from the cluster center were also observed, in each filter and magnification, for sky subtraction purpose. All images are the average of 60 frames of 1 sec integration time. The observations were carried out with seeing $< 1.4''$.

The whole set of data has been analyzed using the package for crowded field photometry ROMAFOT (Buonanno et al. 1979, 1983) and the aperture photometry - PSF fitting correction has been applied.

Eight SAAO standards (kindly provided by Dr. Ian Glass and then published on 1995 by Carter) were observed during the run and most of them at two positions of the array, at least. The calibration curve and details regarding the standard stars were presented in Ferraro et al. (1994). The adopted calibration equations linking the instrumental photometry to the Carter/SAAO system are:

$$K = k + 20.639 \pm 0.010$$
$$J = j + 21.401 \pm 0.030$$

where j and k are the instrumental magnitudes. This error is only due to the linear interpolation of the standard stars; the present calibration uncertainty is entirely dominated by the error due to the aperture photometry - PSF fitting correction, i.e. 0.1 mag in each J and K filter, as already stated by Ortolani et al. (1990). The adopted standard stars don't cover the entire colour range of the NGC6553 data because of the lack of very red standard stars in the Carter standard stars so we had to extrapolate toward colours redder than $(J-K) = 0.84$. The extrapolation is allowed as we do not have colour term in the calibration equations.

HST observations have been obtained through the WFPC2 in February 1994, using the V (F555W) and I (F814W) filters. The exposure times were 2×100 sec. in V and 2×50 sec. in I. Two short exposures in V and I (14 sec. and 5 sec. respectively) have been used for the saturated brightest stars in the deep images.

The data have been calibrated using Holtzman et al. (1995) prescriptions. Their empirical (V, V-I) colour equation has been adopted including the aperture correction provided. Our final transformations from the instrumental fitted magnitudes to the Johnson-Cousins system are:

$$V = v - 0.05(V-I) + 0.027(V-I)^2 + 0.13$$
$$V - I = 1.01(v-i) + 1.98$$

for the exposure frames of 5 sec. in I and 14 sec. in V.

The optical VI sample, coming from HST observations (Ortolani et al. 1995), has been tied to the IR coordinate system using a linear interpolation, and a combined catalogue of 1426 VIJK stars has been created. [1]

[1] The complete table with the results is available on electronic form at the Centre de Données de Strasbourg (CDS) and can be obtained by anonymous ftp copy to cdsarc.u-strasbg.fr (130.79.128.5). The table columns report: 1) the HST identification number where stars between

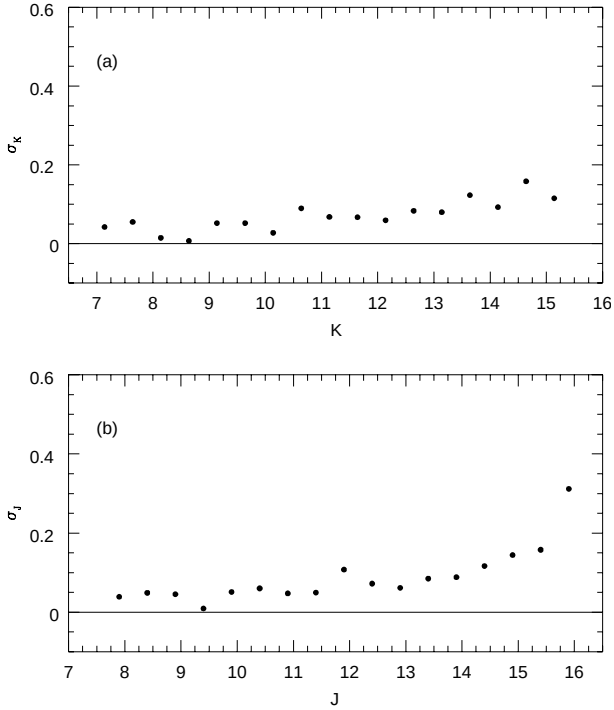

Fig. 2. V (a) I (b) magnitudes and (V-I) (c) colour residuals with respect to the OBB90 for 827 stars in common, plotted versus our magnitudes and colours

Table 1. HST photometric errors

V magnitude	Error
< 17.5	0.03
17.5	0.05
18.5	0.04
19.5	0.04
21.5	0.09
22.5	0.15

Both optical and near-infrared internal photometric errors have been computed from frame to frame comparisons. Concerning the IR data, the internal accuracy of the photometry is shown in Fig. 2, where the median rms scatter, computed over 0.5-mag bins for the stars belonging to the overlapping regions, are plotted versus (a) J and (b) K mean magnitudes. As expected, the median scatter increases at the faintest magnitudes, but it is smaller than 0.1 for most of the objects.

For the HST data, artificial star experiments are not good indicators of the photometric errors because of the well-known difficulties in fitting the PSF. Frame to frame comparison gives the photometric errors in the PC and WF frames, as listed in Table 1 (for final errors divide by a factor $\sqrt{2}$).

1 and 2197 belong to the WFPC2 PC chip, between 20.001 and 26240 to the WFPC2 chip#2, between 30001 and 39545 to the WFPC2 chip #3 while between 40.001 and 48688 to the WFPC2 chip #4; 2) HST V magnitude; 3) HST I magnitude; 4) IRAC2 J magnitude; 5) IRAC2 K magnitude; 6) HST X position transformed to the IRAC2 reference frame and 7) HST Y position.

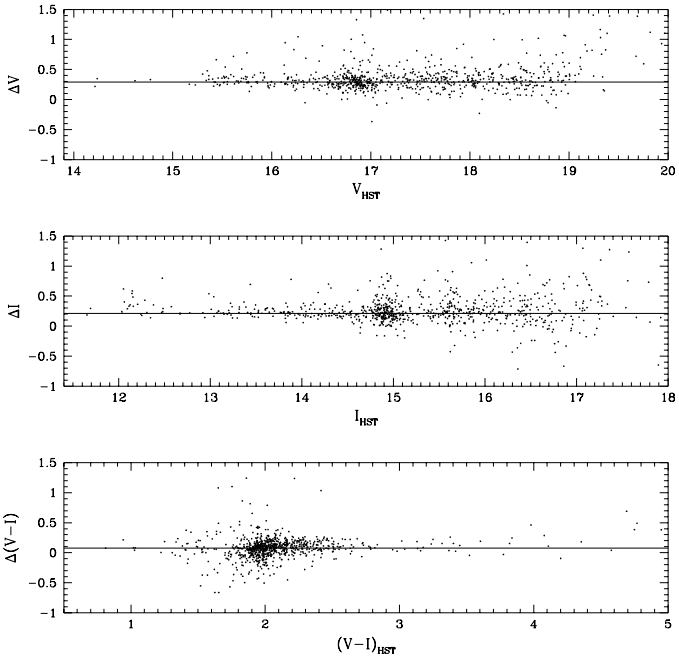

Fig. 3. Median rms scatter of the photometric measures, computed over 0.5-mag bins for stars belonging to the overlapping regions

The I frames have a better signal to noise ratio, yielding a smaller error at the I magnitude corresponding to the V in the CMD. This implies that the photometric errors are dominated by the V magnitudes. Similar photometric errors have been obtained from artificial star experiments.

3. Comparison with previous optical and IR data

Hartwick (1975, hereafter H75) first presented a photographic BV CMD of this cluster. OBB90 presented the CCD BVRI CMDs (1254 stars).

Fig. 3 shows the V and I magnitude and (V-I) colour residuals of the 827 HST stars in common with the OBB90 sample. There is a shift between our data and the previous ones in the sense that the present sample has fainter magnitudes. No indication of a colour trend is present. In particular:

$$V_{HST} - V_{Danish} = 0.292 \pm 0.003$$
$$I_{HST} - I_{Danish} = 0.214 \pm 0.003$$

The positive difference means that our old ground based observations give brighter measurements compared to HST data. In Fig. 3 a clear spread of points toward even higher values is also visible, due to crowding effects in the ground data. The explanation of the systematic error (considering that a comparable difference is present also in the I data) is that the ground based calibration is affected by crowding effects. Our re-analysis of the old data shows that the absolute calibration is correct, and that a new, careful treatment of the aperture magnitude corrections, based on theoretical model stellar profiles (Diego, 1985), gives a final calibration consistent with the new HST data within 0.1

Table 2. Common stars between this paper and Frogel et al. (1983).

Name	J_{Frogel}	K_{Frogel}	J_{IRAC2}	K_{IRAC2}	ΔJ	ΔK	Remarks
I-3	10.74	9.53	10.72	9.57	0.02	-0.04	
II-16	10.51	10.36	10.57	10.32	-0.06	0.04	(1)
II-33	10.84	9.72	10.92	9.85	-0.08	-0.13	(2)
II-44	10.65	9.38	10.56	9.42	0.09	-0.04	
II-54	11.20	10.27	11.71	10.66	-0.51	-0.39	(3)
II-59	9.11	7.69	8.98	7.72	0.13	-0.03	
II-95	10.95	9.74	10.82	9.72	0.13	0.02	
V4	7.78	6.28	7.72	5.77	—	—	(4)
V5	7.87	6.41	8.08	6.36	—	—	(5)

(1) Blended with II-17 only in J filter
II-16 J = 11.43 K = 10.32
II-17 J = 11.23 K = 10.41
J_{tot} = 10.57

(2) Double on IRAC2 frame:
first component J = 11.84 K = 10.87
second component J = 11.52 K = 10.38
J_{tot} = 10.92
K_{tot} = 9.85

(3) Severely crowded

(4) Mira variable, P = 270 d., severely crowded

(5) Long period variable, P = $>$ 100 d., crowded. Out of HST field

mag. To reinforce this point, we have studied the differences between the two set of data with varying brightness and projected stellar density. The results show that the brightest stars have the smallest differences. Moreover the agreement improves in the lowest density regions.

Frogel et al. (1983) presented JHK photoelectric photometry of 9 giants. We have counter-identified all the stars except V5 which is out of the HST field. To allow comparisons with Frogel et al. data sets, magnitudes and colours were transformed to the CIT/CTIO system using the relations by Carter (1993). Table 2 lists: 1) the H75 identification number, 2) and 3) J and K magnitudes from Frogel et al. (1983), 4) and 5) IRAC-2 J and K magnitudes in the CIT/CTIO system, 6) and 7) the difference between magnitudes, 8) remarks. Note the difference in the J filter for the star II-16. In Frogel et al. data, there is a possible blending of this object with star II-17; by simulating the same blending to our data, we get J_{tot} = 10.66, i.d. 0.16 brighter than the previous value. The same applies also for the star II-33 which is blended with a close star. This comparison should be regarded very carefully because of the different observing equipment and always taking into account that this cluster lie in a very crowded and reddened field.

The agreement between the two sets of data is quite good. If stars II-54 (which is severely crowded) and the two variable stars V4 and V5 are not considered, Frogel et al. data are 0.04 $\pm$ 0.04 (J) and -0.03 $\pm$ 0.02 (K) mag fainter than our photometry.

4. The colour magnitude diagram and overall morphology

Figs. 4a and 5a present the CMDs (K, J-K), and (K, V-K) for all sample stars with the mean ridge lines superimposed.

The (V, V-K) CMD is shown in Fig. 6a while Fig. 7a shows, for comparison, the (I, V-I) diagram from the HST sample (Ortolani et al. 1995), containing only the stars in common with the infrared photometry.

In each figure the (a) part represents the whole diagram while the (b) part is a zoom of the horizontal branch region. The positions of all the variable stars, identified from SH73, are superimposed to the relevant evolutionary branches.
The main features of the CMDs are:

– The giant branch is well defined in the whole extension up to K $\sim$ 6.5; a redder spread of points vaguely defining an almost parallel sequence is also visible in all diagrams. Only spectroscopic or a wide field foreground investigation can confirm if this feature is due to a background bulge population. For this reason we have also reduced and analysed the sky frames originally taken only for sky subtraction purposes of the NGC 6553 frames.
Fig. 8 gives the (K, J-K) CMD of one of the sky frames located at $\sim$10′ North from the cluster center. The background field CMD is very similar to that belonging to the Baade Window, published by Davidge (1991). We can notice a feature at $K \sim 13.19$ and $(J-K) \sim 1.0$ similar to a red HB and a clump of blue stars having $K > 13.9$ and $(J-K) < 0.7$ which are probably main sequence stars of a younger component.
To calculate the distance modulus of this field, we have shifted its CMD to match the NGC 6553 data. In particular, the adopted vertical shift is -0.77 mag (in K) which corresponds to the difference in distance between the two objects:
$\Delta(m-M)_{Skyfield-NGC6553}$ = 0.77
Since for NGC 6553, $(m-M)_0$ = 13.6 (see Sect. 8), then $(m-M)_0$ = 14.37 for this sky field, which means an heliocentric distance of 7.5 Kpc in very good agreement with

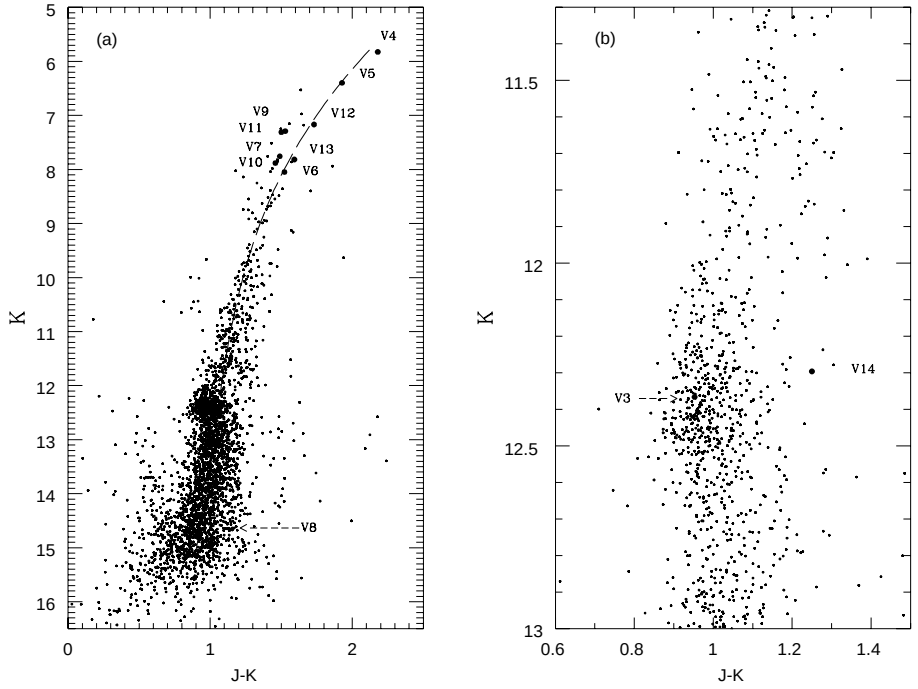

Fig. 4a and b. Infrared (K, J-K) CMD, superimposed is the mean ridge line.

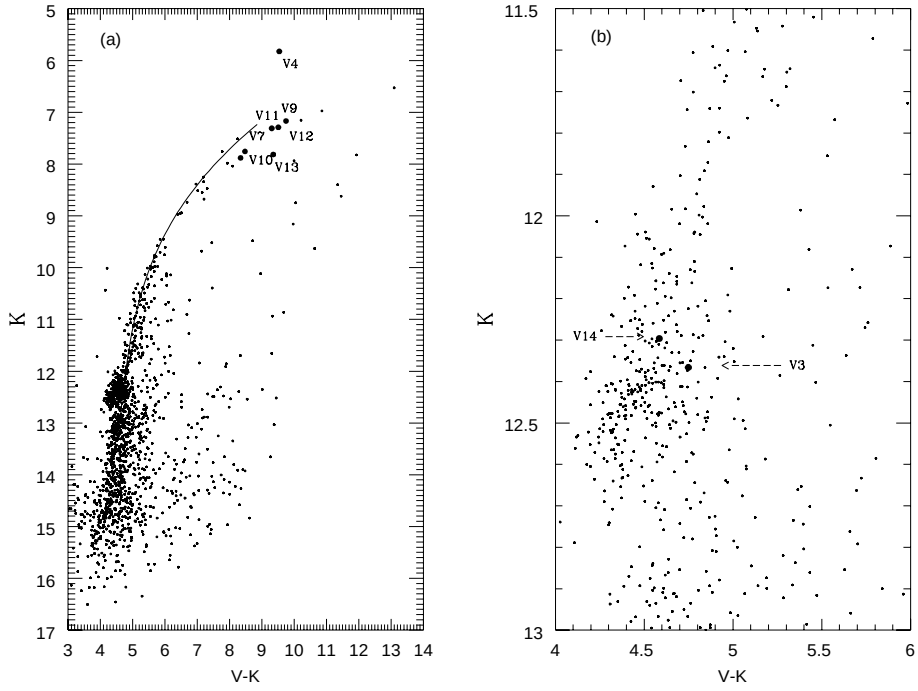

Fig. 5a and b. Composite (K, V-K) CMD with the mean ridge lines superimposed.

the value found by Davidge (1991). The associated error has been calculated from the uncertainties in the differential reddening value, i.e. ± 0.1. This means an error of ± 1 Kpc in the comparison field distance.

To have another estimate we have calculated the differential distance modulus between 47 Tuc and the sky field. From Montegriffo *et al.* (1995), K_{HB} = 11.95 and $(m - M)_0$ = 13.33, so that $\Delta(m-M)_{Skyfield-47\ Tuc}$ = 1.1. As a result, the sky field has $(m - M)_0$ = 14.43 and d = 7.69 Kpc from the Sun. In each case, this is more or less the same distance of the galactic center.

Finally, if the NGC 6553 (K, J-K) CMD is superimposed to the sky CMD, one can notice that some of the above mentioned features are reproduced.

– The steep giant branch in the IR diagrams shows that the use of IR colours greatly reduces the blanketing effects of the cool stars in metal rich clusters. as already shown by Davidge and Simons (1994).
– The positions of the variable stars have been represented with solid circles in all CMDs and in the IR diagram, two mean ridge lines have been superimposed taking or not into

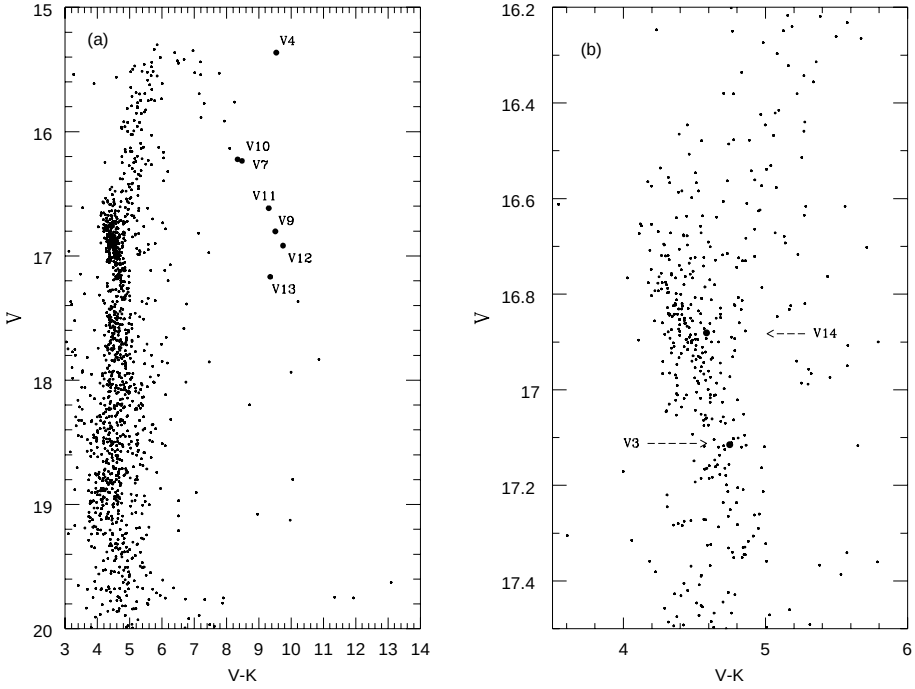

Fig. 6a and b. Composite (V, V-K) CMD.

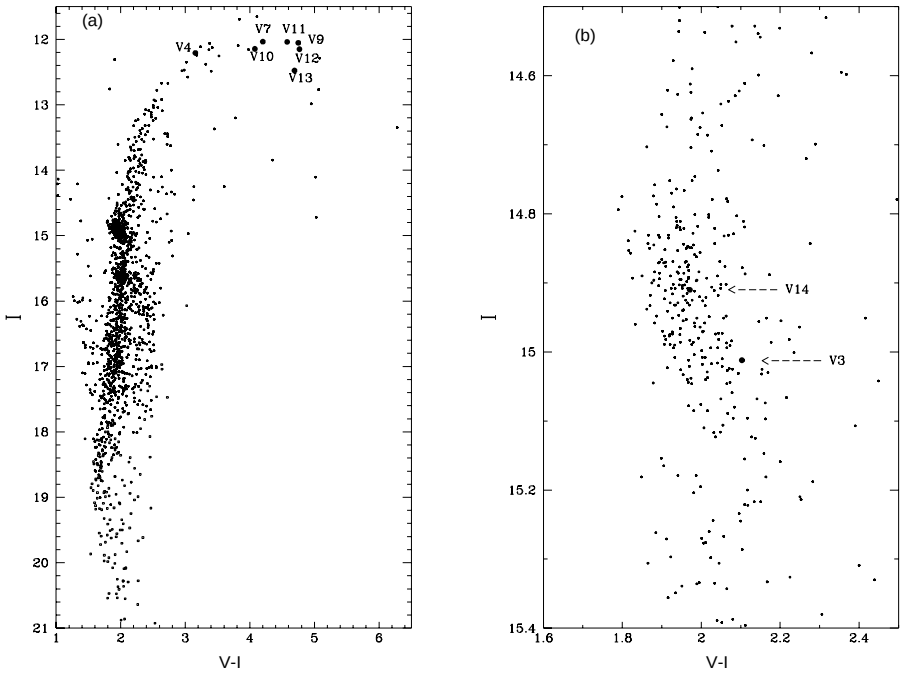

Fig. 7a and b. Composite (I, V-I) CMD only for the stars in common with the infrared sample.

account their presence (solid line and dotted line respectively).

– A clump of points appears in the SGB at V = 17.67 $\pm$ 0.02 and at K = 13.07$\pm$0.01. This could be identified with the so-called "RGB-bump". However, the possibility that it is due simply to a blend with the field background HB cannot be ruled out. Fig. 9 represents the (a) differential and (b) integral K-luminosity function where all the stars belonging to the horizontal branch have been subtracted. The arrow locates the position of the RGB-bump clearly identified also in (b) as a change in the slope of the two dashed lines which are linear fits to the limits of the bump.

– The HB is well defined in all the diagrams and easily identified in Fig. 4 as a well defined clump (see also Davidge and Simons 1994) at about K = 12.42 mag and $(J-K)$ = 0.97, while in Fig. 5 we have $(V-K)$ = 4.5. This measure is much more accurate than the luminosity level obtained using only an optical magnitude on the Y-axis (see Figs. 6a and 6b) or an optical CMDs (see Figs. 7a and 7b) where it appears broadened and strongly tilted. From these values V_{HB} = 16.92 is deduced. The sharpness of the HB in the (K, J-K) diagram

means that the tilting seen in the optical diagrams is not due to the blend of the HB with the SGB bump (for a detailed discussion see Ortolani et al. 1990 and 1992). The obvious conclusion is that differential reddening (or blanketing) is responsible for the tilting in the optical data as suggested by Armandroff (1988) for a number of reddened disk clusters.

5. Variable stars

A comprehensive catalogue of variable stars in globular clusters is given by SH73. To identify their positions, we have used the finding charts of LM73 and H75.

Table 3 lists all the variable stars identified in our sample with respect to SH73, LM73 and H75. The positions of the variable stars (V4, V7, V9, V10, V11, V12, V13) belonging to the giant branch are also shown in all (a) diagrams as filled circles. In each case, Figs. (b) present a zoom of the horizontal branch region where the loci of variables V14 and V3 are identified.

The remaining three variable stars (V5, V6, V8), which do not have a correspondence in the optical sample, because they are out of the HST covered field, are identified in the IR sample as it appears in Table 3.

All the variable stars belonging to the giant branch (AGB) are long period variables (LPVs) and in particular, V4 has been recognized as a Mira star by Andrews et al. (1974) with a period of 265^d. In the (K, J-K) diagram, it is the brightest, and reddest giant star. Also Rosino (1978), includes this star in its list of *Variable stars in Globular Clusters* with a period of 270^d, together with the other long period variable V5 having a period of 100^d as already found by SH73. It is worth mentioning that in Rosino's list, Mira-type variables belonging to globular clusters have a mean period of $< 200.2 \pm 8.9^d$. V4 has, within the Mira-type family, the longest period.

As concerning V3 and V14, they are much fainter and, in principle, they *could* be RR Lyrae stars but this claim has to be tested by means of spectroscopic measurements or well-sampled light curves. Finally, V8 is confirmed to be a field variable star.

6. Cluster parameters

6.1. The bolometric diagram

The infrared photometry allows an accurate determination of the bolometric magnitudes. Using the bolometric corrections by Freedman (1992), namely:
BC_K = 1.97$(J-K)_0$ + 0.92 if $(J-K)_0 < 1.1$
BC_K = 0.70$(J-K)_0$ + 2.32 if 1.1 <= $(J-K)_0 < 1.3$
BC_K = 0.34$(J-K)_0$ + 2.76 if $(J-K)_0 > 1.3$
we derive a bolometric magnitude at the tip of the asymptotic giant branch of m_{bol} = 9.21 corresponding to M_{bol} = −4.66 when a distance modulus of $(m-M)_0$ = 13.6 and $E(B-V)$ = 0.7 mag are assumed (see Sect. 6.3). These values are all affected of an error of ±0.03 mag which takes into account that we have not transformed the magnitudes and colour to the CIT/CTIO system before applying the bolometric corrections. The M_{bol} value is considerably higher than the maximum bolometric magnitude for any old halo cluster (about -3.8) in spite of the moderate integrated visual absolute magnitude of the cluster (M_V = −8.3, see Frogel 1983). If this trend is confirmed, a strong bolometric flux in an old composite stellar population due to the metal rich component is expected. Please refers to Guarnieri et al. 1997a for a detailed discussion of the bolometric diagram.

Moreover, the cluster bolometric luminosity function shown in Fig. 10 is in excellent agreement with the Frogel & Whitford (1987) luminosity function for the bulge (cf. Guarnieri et al. 1997a), an agreement that extends to the brightest stars when allowance is made for the small number statistics in either sample.

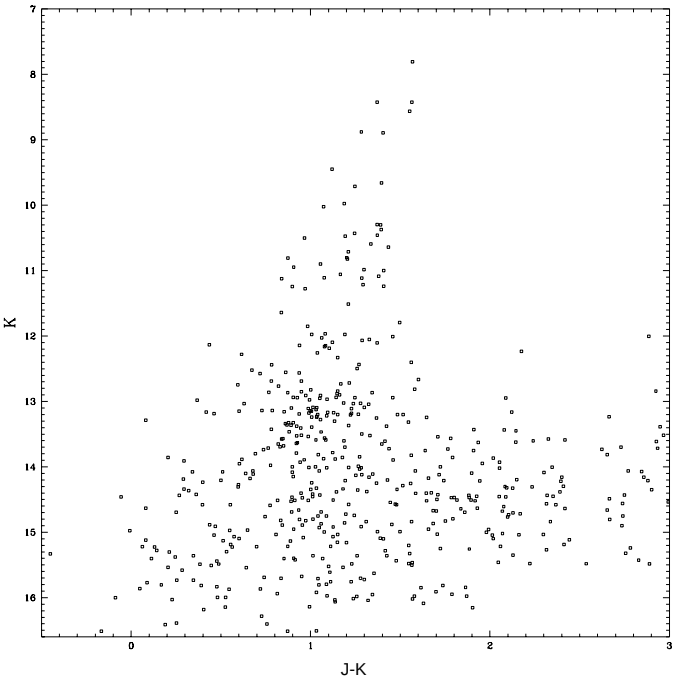

Fig. 8. Infrared (K, J-K) CMD, of one of the external field. Same scale as Fig. 4

6.2. The radial distribution

Figs. 11 represent the (K, V-K) CMDs for annuli at increasing distances from the cluster center. It is quite evident that the K limiting magnitude in Fig. 11b is smaller than that reached in the outer annuli. The structure of the main branches is, anyway, essentially the same. The red region below the dotted line and redder than $V-K \sim 5.5$, includes stars mainly belonging to the main sequence region of Fig. 7 (squares), for which the K magnitude is the result of an artifact of the cross-identification process at faint levels. Local noise peaks have coincided with the position of the star or two close images have not been resolved. The situation is even more complicated by the presence of the background field more evident in Fig. 11d.

Table 3. Variable stars

N_{HST}	V_{HST}	I_{HST}	$V-I$	J_{IRAC2}	K_{IRAC2}	$V-K$	N_{IR}	Var
40127	17.115	15.012	2.103	13.319	12.366	4.749	277	V3
30155	15.364	12.207	3.157	8.004	5.824	9.540	6540	V4
—	—	—	—	8.325	6.397	—	586	V5
—	—	—	—	9.571	8.048	—	581	V6
28	16.235	12.034	4.201	9.246	7.756	8.479	823	V7
—	—	—	—	15.788	14.779	—	1344	V8
40197	16.802	12.052	4.750	8.818	7.290	9.512	713	V9
40198	16.223	12.145	4.078	9.340	7.881	8.342	503	V10
30297	16.616	12.038	4.578	8.810	7.309	9.307	6707	V11
30291	16.917	12.148	4.769	8.899	7.168	9.749	6628	V12
20151	17.168	12.476	4.692	9.407	7.815	9.353	3345	V13
40040	16.881	14.910	1.971	13.546	12.296	4.585	8283	V14

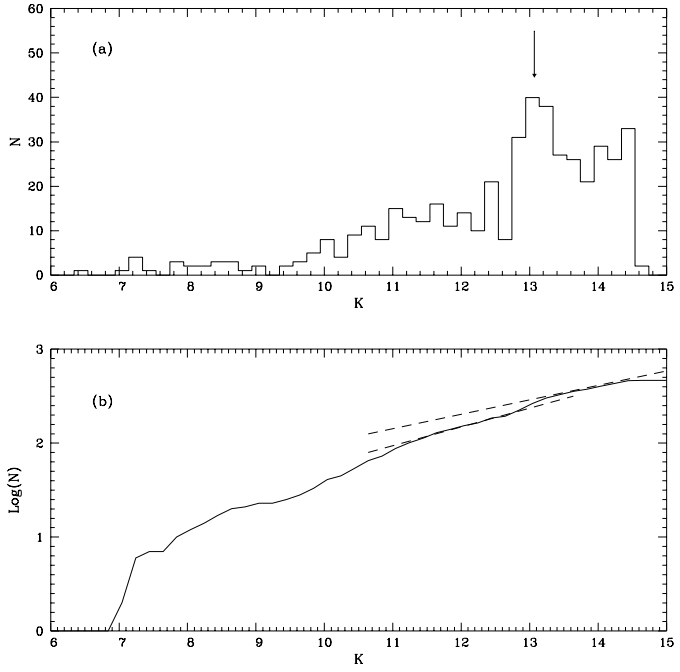

Fig. 9a and b. Luminosity Function

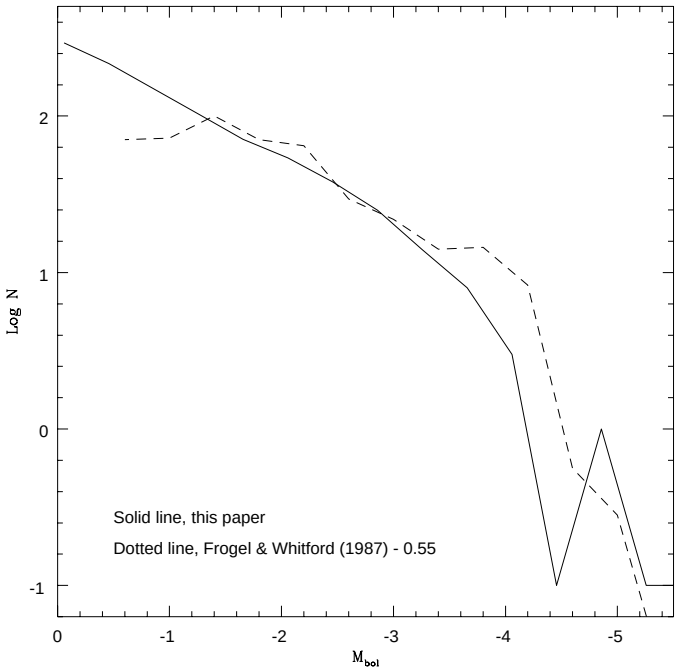

Fig. 10. Bolometric luminosity function, the dotted line represents the Frogel & Whitford bulge luminosity function shifted of 0.55 mag to match our data

6.3. Revised distance and extinction

The precise determination of the distance depends on the assumption for the absolute magnitude of the HB or from the AGB variable stars. This is not easy because, so far, there are no direct measurements of HB for old stars with so high metallicities as that of NGC 6553. Two different approaches can be followed: one is purely theoretical, assuming the absolute magnitude of the HB from the models, and the other, empirical, by extrapolation of lower metallicity determinations.

Assuming the new Padua isochrones (Bertelli et al. 1994), for an age of $\sim$ 14-18 Gyr, the mean level of the horizontal branch is at $M_K = -1.45$, which gives a dereddened distance modulus of 13.4 or about 4.8 Kpc.

Current values for the HB luminosity predict, for $[Fe/H] = -0.2$, absolute visual magnitudes ranging from an upper limit of 0.59 (Y = 0.28, Lee et al. 1990; Sweigart 1987), to 1.23 (Buonanno et al. 1989). Most of these, however, are extrapolated from metal poor samples. Selecting only the relations obtained from nearly solar metallicities, we have M_V = 0.59 (Lee et al. 1990), calculated from theoretical models; M_V = 0.89 (Gratton et al. 1986), derived from an analysis of Baade Window RR Lyrae; M_V = 0.77 (Walker 1992; Chaboyer et al. 1996), from LMC RR Lyrae; and M_V = 1.0 (Jones et al. 1992; Carney et al. 1992) from field, metal rich RR Lyrae.

We adopt an average of $M_V = 0.80 \pm 0.15$, from the last four values, for the NGC 6553 metallicity. An additional ΔV = +0.14 (Johnson, 1966) must be applied to correct the visual magnitude of the RR Lyrae stars ($B - V \sim 0.4$) to the dereddened HB of NGC 6553 ($B - V \sim 0.70$) for the bolometric correction

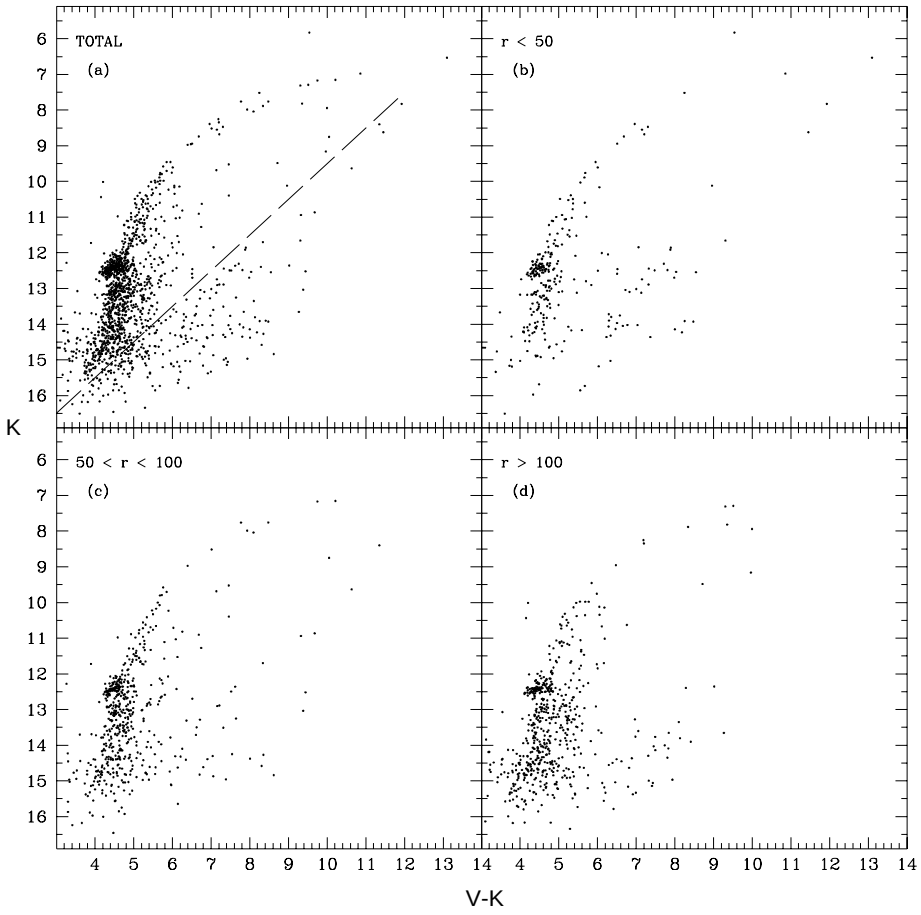

Fig. 11a–d. Radial (K, V-K) CMD. 10a shows the complete sample, whereas 10b, 10c and 10d refers to a subsample inside an annular region of 50 pixels (i.e. 24.5 arcsec), between 50 and 100 (i.e. 49 arcsec) pixels and outside 100 pixels, respectively.

difference. From V_{HB} = 16.92 of NGC 6553 the apparent distance modulus is $(m-M)$ = $16.92-0.8-0.14 = 15.98\pm0.15$

The extinction correction is derived from the fitting of the RGB - SGB with 47 Tuc, once the latter is corrected for a temperature plus blanketing difference due to the metal abundance effect. This effect has been estimated from the mean locus of the globular cluster NGC 6522 (which is projected in the Baade Window) as compared to the background Baade Window population (Barbuy et al. 1994; Terndrup and Walker 1994). From the measured shift of $\Delta(V-I) \sim 0.25$, corresponding to a metallicity difference of [Fe/H] = 0.9, we extrapolate a shift, only due to metallicity, between NGC 6553 and 47 Tuc (Bica et al. 1994) of about $V-I$ = 0.2 mag. An identical result is obtained comparing (B-V) colours. Theoretical models (Bertelli et al. 1994; Vandenberg (1985) predict almost the same amount $(0.15-0.20)$. We use then the observed shift in colour with 47 Tuc, corrected by this metallicity effect to derive the colour excess.

With an observed colour difference of $\Delta(V-I)$ = 1.11 between 47 Tuc and NGC 6553, we obtain a colour excess $E(V-I)$ = 0.95. Assuming a ratio $E(V-I)/E(B-V)$ = 1.35 (Terndrup 1988; Grebel & Roberts 1995) the resulting $E(B-V)$ is 0.7. If we adopt a ratio $A_V/E(B-V)$ = 3.6 (Grebel & Roberts 1995; Olson 1975) we get A_V = 2.5. However, assuming the standard ratio 3.1 (Cardelli et al. 1989; Savage and Mathis 1979), close also to the value recommended for HST photometry (Holtzman et al. 1995), we have A_V = 2.17. The average extinction obtained from these two extremes is A_V = 2.34, corresponding to a distance modulus of $(m-M)_0$ = 13.64 $\sim$ 0.17 and to d = 5.4 Kpc. The ratio $A_V/E(B-V)$ appears as the major source of uncertainty for the distance modulus.

An independent method is based just on IR observations. From the observations of a six globular clusters having a metallicity ranging from $[Fe/H]$ = -2.30 (M30) to $[Fe/H]$ = -0.14 (NGC6528) we roughly get $M_K(HB)$ = $-0.20[Fe/H] - 1.53$ (Guarnieri et al.1997b in preparation), so that M_K = -1.49 for NGC 6553. From its observed $m_K(HB)$ = 12.42 and A_K = $0.38 * E(B-V)$ = 0.27, we have $(m-M)_0$ = 13.64, corresponding to d = 5.35 Kpc.

We finally adopted the unweighted mean of the values, that is $(m-M)_0$ = 13.6 or d = 5.2 Kpc.

6.4. Metallicity

Fig. 12 relates the dereddened colours $(J-K)_0$ and $(V-K)_0$, where are superimposed the 47 Tuc giant stars observed by Frogel et al. (1981 - filled circles) while the dotted line represents the 47 Tuc mean ridge line by Montegriffo et al. (1995). The sequence for the bulge field giants (solid line) is from Frogel et al. (1978). There is a slight shift to higher $(V-K)_0$ values of the NGC 6553 points as compared with 47 Tuc, while the locus

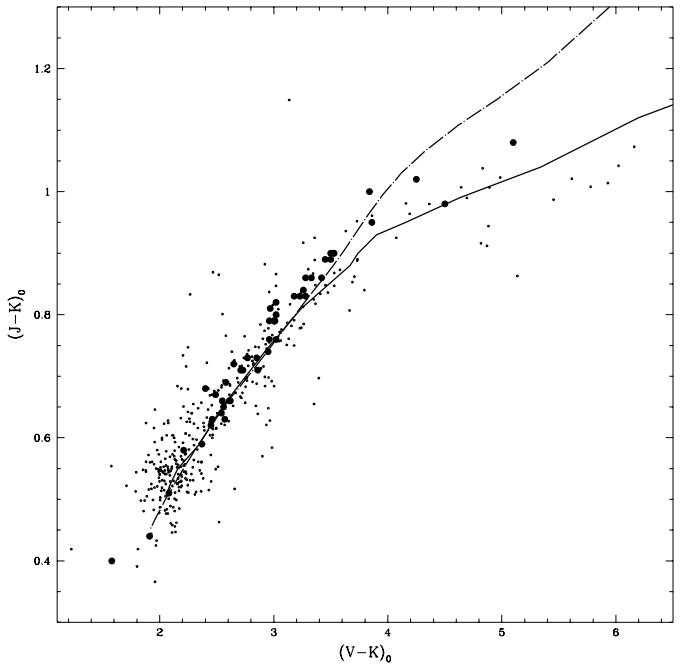

Fig. 12. $(J-K)_0$ vs $(V-K)_0$ colour-colour diagram, the filled stars are from Frogel et al. (1981), the solid line is the sequence for the field giants by Frogel et al. (1978), while the dotted line represent the 47 Tuc mean ridge line (Montegriffo et al., 1995).

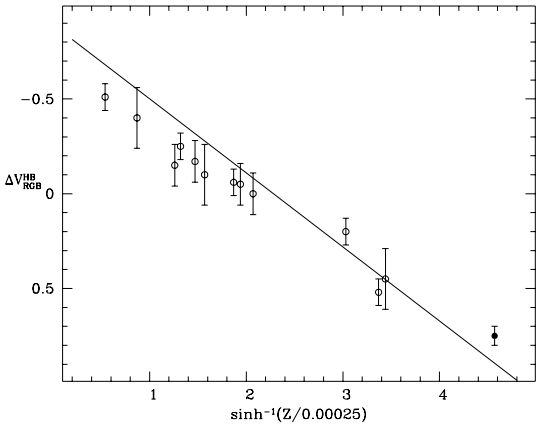

Fig. 13. The $\Delta V_{RGB}^{HB} = 0.33 sinh^{-1}(Z_4/2.5) - 0.68$ relation of Fusi Pecci et al. (1990). Circles represent the metallicity position of the clusters listed in that paper and Ferraro et al. (1994), while the arrow locates the position of NGC 6553.

of the field stars fits NGC 6553 much better. If the shift is only an effect of metallicity (Ferraro et al. 1994; Bertelli et al. 1994) this indicates a metallicity higher than that of 47 Tuc, probably nearly solar, in agreement with Bica et al. (1991). However we should also consider that the recent results from Minniti (1995) are in contrast with a monotonic relation (J-K) vs. metallicity showing instead an apparently random behaviour.

For an independent metal abundance estimation, we also applied the GB slope method of Kuchinski et al. (1995), to the (K, J-K) CMD of NGC 6553, deriving $(GBslope) = -0.117 \pm 0.005$, which corresponds to $[Fe/H] = -0.18 \pm 0.17$ in the Kuchinski et al. calibration. This value is essentially the same ($[Fe/H] = -0.20$) as derived from the high-dispersion analysis of the giant III-17 by Barbuy et al. (1992), and also consistent with the population synthesis results by Santos Jr. et al. (1995).

An updated method to estimate the metallicity in a globular cluster is that of Sarajedini (1994) which, using the $(V-I)_{0,g}$ value of the RGB measured at the level of the HB, and the difference $\Delta V_{1.2}$ in V between the HB and the RGB at $(V-I)_0 = 1.2$, derives its value via the equations:

$[\mathrm{Fe/H}] = 9.668 \times [(\mathrm{V-I})_{0,\mathrm{g}} - \mathrm{E(V-I)}] - 10.64$

$[\mathrm{Fe/H}] = -0.9367 \times \Delta \mathrm{V}_{1.2} + 0.2606$

The reddening value $E(V-I)$ is simultaneously derived.

By applying such a method to NGC 6553 we obtained <[Fe/H]>= -0.28 ± 0.15 and $E(V-I) = 0.99$ which corresponds to $E(B-V) = 0.76$ consistent both with OBB90 and with the previous value.

The unweighted mean of the metallicity is $[Fe/H] = -0.22 \pm 0.05$ which can be adopted as the average value of the cluster metal abundance.

As a further check, we have plotted, in Fig. 13, the value of the inverse hyperbolic sine of this metallicity versus the difference in the V magnitude between the horizontal branch and the mean locus of the RGB-bump as described in Fusi Pecci et al. (1990). The arrow locates the position of the NGC 6553 metallicity while the other values are taken from Fusi Pecci et al. (1990) and Ferraro et al. (1994). As can be seen, NGC 6553 fits well the relation.

6.5. Star counts and the helium abundance

Because of the above mentioned difficulties in separating the AGB from the RGB, the R' method has been applied to derive the helium abundance. The ratio of the GB plus AGB to HB stars is 1.46 from counts in the (K, J-K) diagram of Fig. 4. The same ratio calculated from Fig. 5 (K, V-K) gives 1.56. A third value was obtained from the optical HST data (R' = 1.41), in excellent agreement with the IR ground based results. Assuming an average of R'=1.48, a helium abundance of 0.28 is derived from Buzzoni et al. (1983), clearly above the average of the abundance discussed by these authors. This value is in very good agreement Minniti (1995) which found a mean He abundance of the Galactic bulge of $Y = 0.28 \pm 0.02$ by observing several bulge fields on the K filter.

While the absolute helium abundance is strongly dependent on the model assumption and several parameters (e.g., semiconvection, overshooting, age) it is clear that NGC 6553 presents a higher R' number when compared to metal poor halo clusters. Minniti (1995) and Tiede et al. (1995) arrived to the same numbers from IR observations obtained in several bulge fields. Different results at very low and very high values have been previously obtained by Terndrup (1988), in the optical (Y=0.30) and by Davidge (1991), from IR data ($Y \leq 0.22$), in the Baade Window field.

7. Conclusions

We have presented JK infrared photometry combined with high resolution visual observations, for the low-latitude, high metallicity, bulge globular cluster NGC 6553.

The advantages in combining infrared and HST optical data are evident in all the presented CMDs, with a greatly reduced foreground contamination and a limited effect of differential reddening (due to the relatively much higher sensitivity of the temperature to the chosen colour indices). Moreover, the combination infrared and optical colours leads to more accurate temperature determinations, which is fundamental for spectroscopic analyses of these globular cluster giants.

The JK diagram confirms the peculiarities of the metal rich, old population, with a very bright AGB tip reaching $M_K = -8.04$ for the brightest long period variable star. Converted to bolometric magnitudes this means $M_{bol} = -4.66$ which is almost two magnitudes higher than in M92 and 47 Tuc (Freedman 1992). Combined with the finding of an old age (Ortolani et al. 1995) this makes the brightest stars of NGC 6553 in the infrared, blanketing-free bands, also the brightest among evolved stars.

The revised distance (R=5.2 Kpc) is not substantially different from the values found by OBB90 and confirm the bulge membership of this cluster. Also the reddening ($E(B-V) = 0.7$) and metallicity values ($[Fe/H] = -0.22$) are very close to the previous estimations. Finally the helium abundance derived through the R'-method ($Y = 0.28$) is consistent with the almost solar metal abundance and with the field population value.

Acknowledgements. We would like to thank the ESO organization for the allocation of observing time and for giving us the chance to be the first IRAC-2 users. We also thank Hans Gemperlein for the help during the observing run and Francesco R. Ferraro for many helpful discussions and suggestions that resulted in a significantly better presentation. MDG acknowledges the Università and Osservatorio Astronomico of Torino for their support.

References

Andrews, P.J., Feast, M.W., Lloyd Evans, T., Thackeray, A.D., & Menzies, J.W. 1974, The Observatory, 94, 133
Armandroff, T.E. 1988, AJ, 96, 588
Barbuy, B., Castro, S., Ortolani, S., & Bica, E. 1992, A&A, 259, 607
Barbuy, B., Ortolani, S., & Bica, E. 1994, A&A, 285, 871
Bertelli, G., Bressan, A., Chiosi, C., Fagotto, F., & Nasi, E. 1994, A&AS, 106, 275
Bica, E., Barbuy, B., & Ortolani, S. 1991, ApJ, 382, L15.
Bica, E., Ortolani, S., & Barbuy, B. 1994, A&AS, 106, 161
Buonanno, R., Corsi, C.E., De Biase, G.A., & Ferraro, I. 1979, in Image processing in Astronomy, eds. G. Sedmak, M. Capaccioli and R.J. Allen, Trieste Obs., 354
Buonanno, R., Buscema, G., Corsi, C.E., Ferraro, I., & Iannicola, G. 1983, A&A, 126, 278
Buonanno, R., Corsi, C.E., & Fusi Pecci, F. 1989, A&A, 216, 80
Buzzoni, A. 1993, A&A, 275,433.
Carney, B.W., Storm, J., & Jones, R.V. 1992, ApJ, 386, 663
Cardelli, J.A., Clayton, G.C., & Mathis, J.S. 1989, ApJ, 345, 245
Carter, B.S. 1993, in Precision Photometry, eds. D. Kilkenny, E. Lastovica & J.W. Menzies, (Cape Town: SAAO), 100
Carter, B.S. 1995, MNRAS, 276, 734
Chaboyer, B., Demarque, P., Kernan, P.J., & Krauss, L.M. 1996, Science, 271, 957
Davidge, T.J. 1991, ApJ, 380,116
Davodge, T.J., Simons, D.A. 1994, AJ, 107, 240
Diego, F. 1985, PASP, 97, 1209
Ferraro, F.R., Fusi Pecci, F., Guarnieri, M.D., Moneti, A., Origlia, L., & Testa, V. 1994, MNRAS, 266,829
Freedman, W.L. 1992, AJ, 104, 1349.
Frogel, J.A., 1983, ApJ, 272, 167
Frogel, J.A., Cohen, J.G., & Persson, S.E. 1983, ApJ, 275, 773
Frogel, J.A., Persson, S.E., Aaronson, M., & Matthews, K. 1978, ApJ, 220,75
Frogel, J.A., Persson, S.E., & Cohen, J.G. 1981, ApJ, 246,842
Fusi Pecci, F., Ferraro, F.R., Crocker, D.A., Rood, R.T., & Buonanno, R. 1990, A&A, 238,95
Gratton, R., Tornambè, A., & Ortolani, S. 1986, A&A, 169,111
Grebel, E.K., & Roberts, W.M. 1995, A&AS, 109, 293.
Guarnieri, M.D., Fusi Pecci, F.,& Ferraro, F.R. 1992, Mem.S.A.It., 63, 117
Guarnieri, M.D., Renzini, A., Ortolani, S. 1997a, ApJ 477, L21
Guarnieri, M.D., Ortolani, S., Renzini, A., 1997b, in preparation
Hartwick, F.D.A. 1975, PASP, 87, 77 (H75)
Holtzman, J.A., Burrows, C.J., Casertano, S. et al. 1995, PASP, 107, 1065
Johnson, H.L. 1966, ARA&A, 4, 193
Jones, R.V., Carney, B.W., Storm, J., & Latham, D.W. 1992, ApJ, 386, 646
Kuchinski, L.E., Frogel, J.A., & Terndrup, D.M. 1995, AJ, 109, 113
Lee, Y.-W., Demarque, P., & Zinn, R. 1990, ApJ, 350, 155
Lloyd Evans, T., & Menzies, J.W. 1973, in Variable stars in Globular Clusters and Related Systems, IAU Coll. 21, ed. J.D. Fernie, Reidel, Dordrecht, 151 (LM73)
Minniti, D. 1995, A&A, 300, 109
Montegriffo, P., Ferraro, F.R., Fusi Pecci, F., & Origlia, L., 1995, MNRAS, 276, 739
Moorwood, A., Finger, G., Biereichel, P., Delabre, B., Van Dijsseldonk, A., Huster, G., Lizon, J.-L., Meyer, M., Gemperlein, H., & Moneti, A. 1992, The Messenger, 69,61
Olson, B.I. 1975, PASP, 87, 349
Ortolani, S., Barbuy, B., & Bica, E. 1990, A&A, 236,362 (OBB90)
Ortolani, S., Bica, E., & Barbuy, B. 1991, A&A, 249, L31
Ortolani, S., Barbuy, B., & Bica, E. 1992, A&AS, 92, 441
Ortolani, S., Barbuy, B., & Bica, E. 1993a, A&A, 273, 415
Ortolani, S., Barbuy, B., & Bica, E. 1993b, A&A, 267, 66
Ortolani, S., Renzini, A., Gilmozzi, R., Marconi, G., Barbuy, E., Bica, E. & Rich, R.M. 1995, Nature, 377, 701
Raha, N., Sellwood, J.A., James, R.A., & Kahn, F. D. 1991, Nature, 352, 411
Rosino, L. 1978, Vistas in Astr. 22, 39
Santos Jr., J., Bica, E., Dottori, H., Ortolani, S., & Barbuy, B. 1995, A&A, 303, 753
Sarajedini, A. 1994, AJ, 107, 618
Savage, B.D., & Mathis, J.S. 1979, ARA&A, 17, 73
Sawyer Hogg, H. 1973, Publ. David Dunlop Obs., 3, n.6. (SH73)
Sweigart, A.V. 1987, ApJS, 65, 95
Terndrup, D.M. 1988, AJ, 96, 884
Terndrup, D.M., & Walker, A.R. 1994, AJ, 107, 1786
Tiede, G.P., Frogel, J.A., & Terndrup, D.M. 1995, AJ, 110, 2788
Vandenbergh, D. 1985, ApJS, 58, 711
Walker, A.R. 1992, ApJ, 390, L81